On-line identification of diastereomeric dibenzo[a,l]pyrene diol epoxide-derived deoxyadenosine adducts by capillary electrophoresis-fluorescence line-narrowing and non-line narrow...

ARTICLE *in* JOURNAL OF CHROMATOGRAPHY A · SEPTEMBER 1999

Impact Factor: 4.17 · DOI: 10.1016/S0021-9673(99)00507-5 · Source: PubMed

ELSEVIER

Journal of Chromatography A, 853 (1999) 159–170

JOURNAL OF CHROMATOGRAPHY A

On-line identification of diastereomeric dibenzo[*a,l*]pyrene diol epoxide-derived deoxyadenosine adducts by capillary electrophoresis–fluorescence line-narrowing and non-line narrowing spectroscopy

Kenneth P. Roberts, Cheng-Huang Lin[1], Ryszard Jankowiak*, Gerald J. Small

Ames Laboratory – US Department of Energy and Department of Chemistry, Iowa Sate University, Ames, IA 50011, USA

Abstract

A capillary electrophoretic method for the separation and on-line identification of closely related analytes using low-temperature fluorescence spectroscopy is reported for the eight diastereomeric deoxyadenosine (dA) adducts derived from dibenzo[*a,l*]pyrene diol epoxide (DB[*a,l*]PDE). Electrophoretic separation of stereoisomers was accomplished by application of a mixed surfactant buffer [dioctyl sulfosuccinate (DOSS) and Brij-S], which was below the critical micelle concentration (CMC) due to the high concentration (~25%) of organic solvent. Addition of multiple surfactant additives to the separation buffer provided electrophoretic resolution, which was unattainable under single surfactant conditions. It is shown that the CE-separated analyte zones could be identified on-line via low-temperature (4.2 K) fluorescence non-line narrowing and fluorescence line-narrowing (FLN) spectroscopy. In addition, it was determined that in CE buffer *trans-syn-*, *cis-syn-* and *cis-anti*-DB[*a,l*]PDE-14-N^{6}dA diastereomeric adducts exist mostly with the –dA and DB[*a,l*]P moiety in an ''open''-type conformation while the *trans-anti*-DB[*a,l*]PDE-14-N^{6}dA adducts exist in two different conformations whose relative distribution depends on matrix composition. The above conformations have also been revealed by selective laser excitation. Thus, the low-temperature methodology not only provides fingerprint structure via vibrationally resolved 4.2 K fluorescence spectra for adduct identification, but also provides conformational information on the spatial relationship of the carcinogen and dA moiety. These results, taken together with those for DB[*a,l*]P–DNA adducts formed in standard glasses and mouse epidermis exposed to DB[*a,l*]P, support our earlier findings that DB[*a,l*]P-derived adducts exist in different conformations [Jankowiak et al., Chem. Res. Toxicol. 11 (1998) 674]. Therefore, the combination of the separation power of CE and spectral selectivity of low-temperature fluorescence spectroscopy at NLN and FLN conditions provides a powerful methodology which should prove useful for identification of closely related DNA adducts formed at low levels in biological systems.

Keywords: Detection, electrophoresis; Fluorescence detection; Fluoresence line narrowing spectroscopy; Fluoresence non-line narrowing spectroscopy; Deoxyadenosine; Dibenzopyrene diol epoxide; DNA; Polynuclear aromatic hydrocarbons

1. Introduction

The polycyclic aromatic hydrocarbons are an important class of carcinogen. They are activated by two main pathways: one-electron oxidation to yield radical cations [1–4] and monooxygenation to

*Corresponding author. Tel.: +1-515-2944-394; fax: +1-515-2940-105.

E-mail address: jankowiak@ameslab.gov (R. Jankowiak)

[1]Present address: Chaoyang University of Technology, Department of Applied Chemistry, 168 Gifeng E. Road, Wufeng, Taichung County, Taiwan.

0021-9673/99/$ – see front matter
PII: S0021-9673(99)00507-5

produce bay region diol epoxides [5–10] which react with the nucleophilic centers of DNA bases, particularly those associated with guanine and adenine. It is widely accepted that the formation of DNA–PAH adducts is the initial event that leads to mutations that result in cancer [11,12]. In this paper we present results on DNA adducts formed from dibenzo[*a,l*]pyrene (DB[*a,l*]P) the most potent member of the PAH class of carcinogens [13,14]. It is found in river sediment [15] and indoor/outdoor air samples [16,17]. The technique used to obtain the results was capillary electrophoresis–fluorescence line narrowing spectroscopy (CE–FLNS) which has recently been developed by our laboratory [18]. The technique allowed, for the first time, on-line structural characterization of DNA–carcinogen adducts. Capillary electrophoresis can also be interfaced with non-line narrowed fluorescence (NLNF) spectroscopy.

Prior to our development of CE–FLNS we had employed high-performance liquid chromatography (HPLC) with FLNS to characterize and quantitate a wide variety of DNA–PAH adducts in an off-line mode. The results obtained, when combined with the results of computational chemistry had shown that DB[*a,l*]P leads to a diverse spectrum of stable DNA adducts formed by the diol epoxide metabolic pathway [19]. Conformational information has been obtained for DB[*a,l*]PDE-14-N7Ade, –N7Gua [20], DB[*a,l*]P tetrols [21], and various DB[*a,l*]PDE-14-N^6deoxyadenosine (dA) stereoisomeric adducts [22,23]. It was shown that *anti*- and *syn*- derived DB[*a,l*]PDE-14-N^6dA adducts in ethanol and glycerol–water glasses can adopt various ''open''- and ''folded''-type conformations between the dA and carcinogen moiety; only the folded conformation allows significant interactions between the dA and aromatic portion of the carcinogen [23].

Off-line fluorescence studies, however, indicated that in some instances the purity of the DB[*a,l*]PDE-derived adducts being analyzed poses a problem, especially if the analytes are unstable and/or cannot be HPLC baseline resolved. To circumvent this problem we developed and applied the methodology, which interfaces CE with FLNS for on-line spectral characterization and identification of these closely related species. It has been shown that CE-separated fluorescent analytes can be identified on-line via fingerprint structure of vibrationally resolved FLN spectra at 4.2 K [18,24,25].

CE has also been coupled to mass spectrometry (MS) and nuclear magnetic resonance (NMR) for on-line analyte characterization. Both have yielded interesting results without the requirement of standards present for analysis, although some difficulties exist [26–32]. In the case of CE–MS some of the issues have been circumvented with the introduction of capillary electrochromatography (CEC) [33–35]. CEC incorporates the packed stationary phase of LC (minimizing the need for surfactants) and the efficient electroosmotic flow mechanism of CE.

In this respect, we note that FLNS can also be coupled with CEC [36], and emphasize that the CE–FLNS approach mentioned above does not require standards each time a qualitative determination is to be made, but relies on an established reference library of spectra. This attribute of CE–FLNS is particularly important in the biomedical/biochemical sciences, where many standards (e.g., DNA and protein adducts/metabolites) are difficult/expensive to synthesize, and/or possess poor stability over time. These features of CE–FLNS, along with arbitrary detection times, selective determination in the frequency and time space, as well as increased fluorescence signal and/or decreased photodegradation (due to the low temperatures used), indicate that CE–FLNS is an appropriate methodology for identification, characterization and quantitation of closely related analytes [18,24,25].

To complement the CE–FLNS methodology, it is shown here that adduct identification can also be achieved via CE and low-temperature fluorescence spectra obtained under non-line-narrowing conditions. With this approach expensive tunable lasers are not required, i.e., a single-frequency excitation source can be used, expanding the applicability of low-temperature wavelength-resolved laser-induced fluorescence (LIF) detection in capillary electrophoresis [37]. Utilization of low-temperature in obtaining LIF spectra provides spectral resolution that is not possible at room temperature. At room temperature, fluorescence signals are spectrally broad and often featureless, rendering them useless for identification purposes due to the nearly identical emission spectra of structurally similar analytes. In CE–FNLN spectroscopy, reduction in sample temperature to 4.2

K effectively eliminates thermal broadening contribution, which for a single vibronic transition is approximately equal to kT~200 cm^{-1} at room temperature. In the case of FLNS, a further reduction in line-width by a factor of 10–100 is achieved by selective excitation of a uniform subset of molecules [3,38,39]. The selective excitation eliminates inhomogeneous broadening which is typically about 100–500 cm^{-1} in amorphous solids [39].

In this paper, we report on the separation of eight DB[*a,l*]PDE-14-N^6dA diastereomeric adducts (see Fig. 1), and their on-line identification via low-temperature NLN fluorescence spectra. An example of analyte identification via FLN spectra is also shown for completeness. The main goal, however, is to establish a protocol for the separation and spectral characterization of closely related diastereomeric DB[*a,l*]PDE-derived dA adduct standards in CE buffer, and to provide a library of the NLN spectral fingerprints for future on-line in vivo and in vitro studies of –dA adducts derived from DB[*a,l*]P by CE–FNLN/FLN.

2. Experimental

Caution. *anti*- and *syn*-DB[*a,l*]P diol epoxides are extremely hazardous chemicals and should be handled carefully in accordance with NIH guidelines.

2.1. Materials

Sodium tetraborate (STB), sodium dioctyl sul-

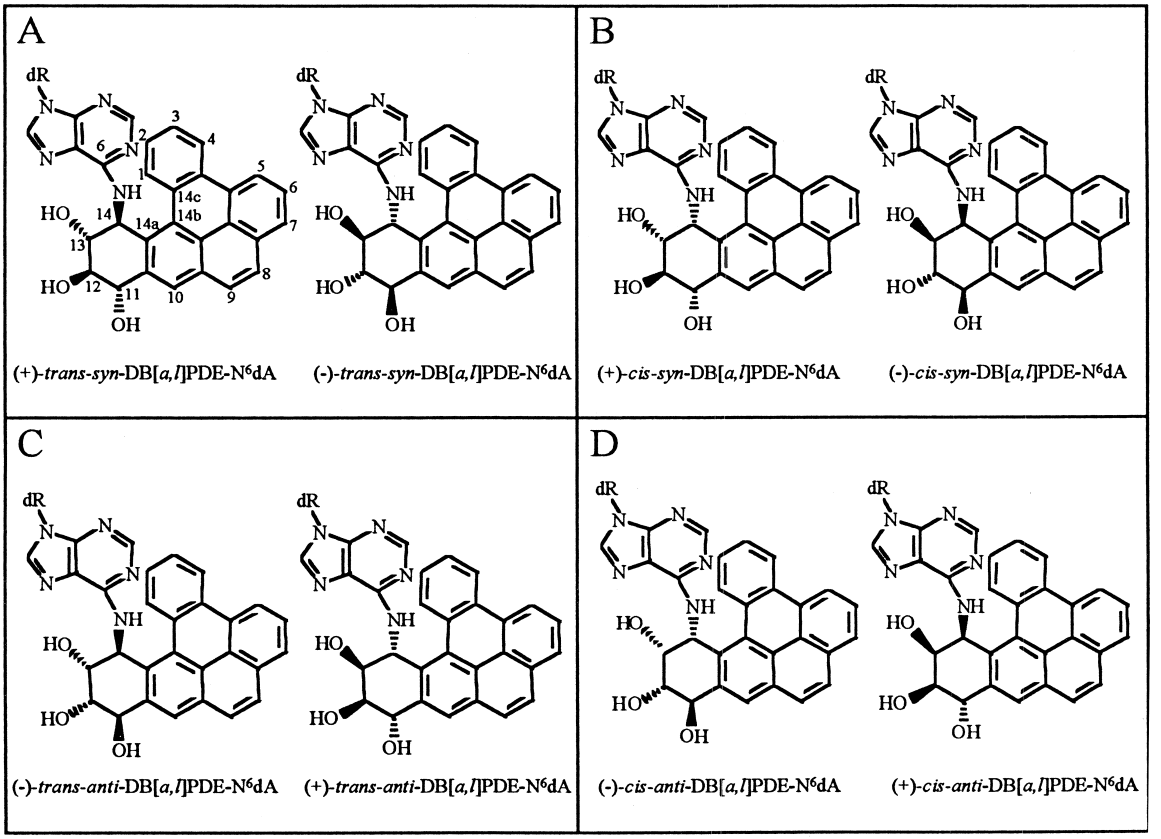

Fig. 1. Molecular structures of the eight DB[*a,l*]PDE-14-N^6dA adducts investigated: (A) (±)-*trans-syn*-DB[*a,l*]PDE-14-N^6dA; (B) (±)-*cis-syn*-DB[*a,l*]PDE-14-N^6dA; (C) (±)-*trans*-anti-DB[*a,l*]PDE-14-N^6dA; and (D) (±)-*cis-anti*-DB[*a,l*] PDE-14-N^6dA. dR corresponds to deoxyribose.

fosuccinate (DOSS) and Brij 30 were obtained from Aldrich (Milwaukee, WI, USA). Acetonitrile (ACN) and sodium hydroxide (NaOH) were obtained from Fisher Scientific (Fair Lawn, NJ, USA). All buffers were prepared with water purified with a NANOpure II (Barnstead, Dubuque, IA, USA) purification system. Capillaries were 75 μm I.D.×375 μm O.D. UV-transparent bare silica purchased from Polymicro Technologies (Phoenix, AZ, USA). Glycerol was obtained from Spectrum Chemical Mfg. (Gardena, CA, USA).

2.2. Sample preparation and buffers

The DB[*a,l*]PDE derived stereomeric adducts *trans-anti-*, *cis-anti-*, *trans-syn-* and *cis-syn*-DB[*a,l*]-PDE-14-N^6dA were synthesized by a reaction of *anti-* and *syn*-DB[*a,l*]PDE with dA. The (±)-*anti*-DB[*a,l*]PDE was reacted with optically-active dA in dimethylformamide at 100°C for 30 min to give four diastereomeric *anti*-DB[*a,l*]PDE-14-N^6dA adducts. Likewise, the (±)-*syn*-DB[*a,l*]PDE was reacted with optically-active dA under the same conditions, to yield the four *syn*-DB[*a,l*]PDE-14-N^6dA diastereomeric adducts. Further details on the synthesis and structural characterization are described elsewhere [22].

The CE buffer consisted of an ACN–water solution (25.5%, v/v) containing 34 m*M* DOSS, 7.5 m*M* Brij-S (sulfonated Brij 30 as described by Ding and Fritz [40]), and 6.8 m*M* sodium tetraborate to form a mixed surfactant solution. Aqueous NaOH was used to adjust the pH to 9. Before injection, the separation buffer was filtered through a 0.22 μm syringe filter (Costor) and then degassed for 5 min.

Matrix dependent (off-line) studies of the dA standards at 77 and 4.2 K were performed in both 100% CE buffer and CE buffer–glycerol (20:80, v/v) to determine how the matrix affected the conformational distribution of the stereoisomers. Samples were diluted to equal concentrations in the appropriate matrix, placed in 2-mm I.D. quartz tubes, and brought to 4.2 K for LIF measurements. Approximately 20 μl sample volumes were sufficient for the off-line analysis.

2.3. Instrumentation

A schematic of the CE–FLN/FNLN system is shown in Fig. 2. A modular capillary electrophoresis system (Crystal 300 series, Model 310, ATI Unicam, Boston, MA, USA) was used for the electrokinetic separations. Capillaries were 85 cm (75 cm effective length) for LIF detection. Capillaries were conditioned with 100 m*M* NaOH for 15 min (30 min for new capillaries), water for 5 min, and separation buffer for 15 min. The sample was hydrodynamically injected with 20 mbar pressure for 3 s resulting in approximately a 10 nl injection volume. Separations were carried out at 20 kV resulting in a 40 μA current.

Room-temperature, LIF electropherograms were obtained with a CW excitation source (Model Innova 90C argon ion laser, Coherent, Santa Clara, CA, USA) equipped with UV optics and an intracavity prism for single line selection. Pulsed excitation was accomplished with a Lambda Physik FL-2002 dye laser, pumped by a Lambda Physik Lextra 100 XeCl excimer laser (Lambda Physik, Fort Lauderdale, FL, USA). When the molecules of interest electrokinetically migrated into the observation window, the temperature of the capillary, housed in a specially designed capillary cryostat (CC) [18,24,25], was reduced to 4.2 K for low-temperature, on-line analysis. The cooling process took less than 1 min. Individual analyte zones in the capillary were selectively probed by automated translation of the CC. Fluorescence was collected with a specially designed objective (Ealing, Holliston, MA, USA), passed through a Model 218 0.3 m monochromator (McPherson, Acton, MA, USA), and detected with an intensified CCD camera (Princeton Instruments, Trenton, NJ, USA) using gated and non-gated modes of detection. Spectral resolution for FLN and NLN were 0.05 and 0.8 nm, respectively. Further details of the experimental set-up are given in Ref. [18].

3. Results and discussion

3.1. Off-line NLN fluorescence spectra in CE buffer

In this section we present NLN fluorescence spectra obtained using a CE buffer in order to determine whether or not the spectra allow for distinction between the isomers of *anti-* and *syn*-DB[*a,l*]PDE-14-N^6dA.

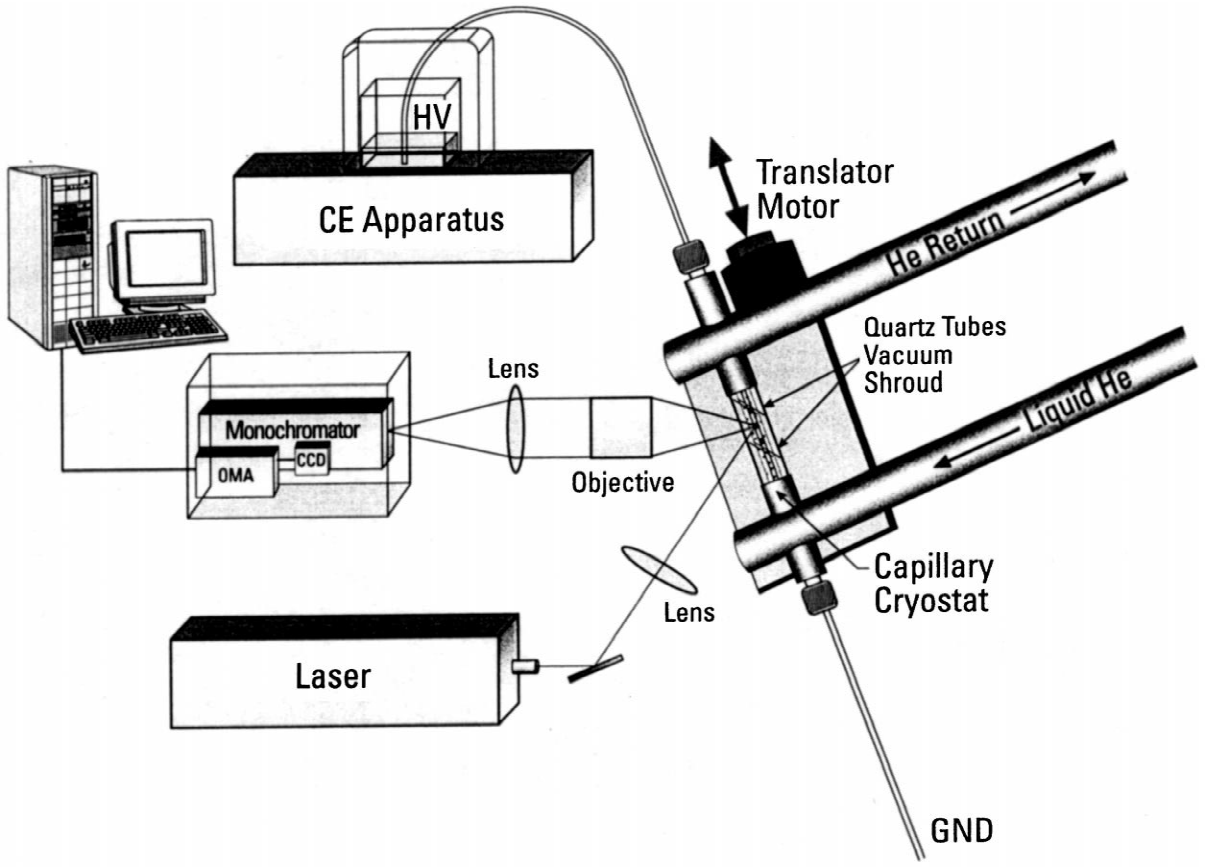

Fig. 2. Schematic apparatus of the CE–FLNS system used for structural characterization of CE-separated analytes.

A reference library was established for the DB[*a,l*]PDE-14-N^{6}dA adducts in CE buffer, as shown in Fig. 3. Spectra a–d, correspond to the (−)-*trans-anti-,* (−)-*cis-anti-,* (+)-*trans-syn-,* (+)-*cis-syn*-dA adducts, respectively. Identical spectra for the corresponding optical conjugates were obtained (not shown). However, the NLN spectra of the above four stereoisomeric adducts are clearly distinguishable, and can therefore be used for on-line identification of DB[*a,l*]PDE-derived deoxyadenosine adducts.

As shown in spectrum a, the (−)-*trans-anti*-dA adduct (in CE buffer) favors a conformation with a (0,0) origin band at 383.5 nm, in sharp contrast to the spectra obtained recently in ethanol and glycerol–water glasses where the major origin band of the same adduct was red-shifted to ~388 nm [23]. This large shift cannot be accounted for by simple matrix-dependent spectral shifting. Rather, it is due to matrix-induced conformational changes [20,21]. This is supported by the fact that a minor conformation, with an origin band at ~383 nm, was also observed in an ethanol matrix (see Table 1). The remaining adducts spectra (b, c and d), though all in conformation I, still reveal significant differences in their S_0 vibronic intensity distribution. The origin bands of the adducts discussed above are summarized in Table 1. The observed variations in the vibronic intensity distribution are not surprising given that the parent fluorophore B[*e*]P has C_{2v} symmetry, and the out of plane deformation, as well as the conformation of the cyclohexenyl ring depend on adduct stereochemistry [41,42]. Furthermore, the significant intensity of the 770, 790 and 780 cm^{-1} bands in spectra b, c and d, respectively, of Fig. 3 are due to electronic–vibrational coupling between the S_1 state and higher energy dipole-allowed states, and is a consequence of the $S_1 \leftarrow S_0$ absorption transition

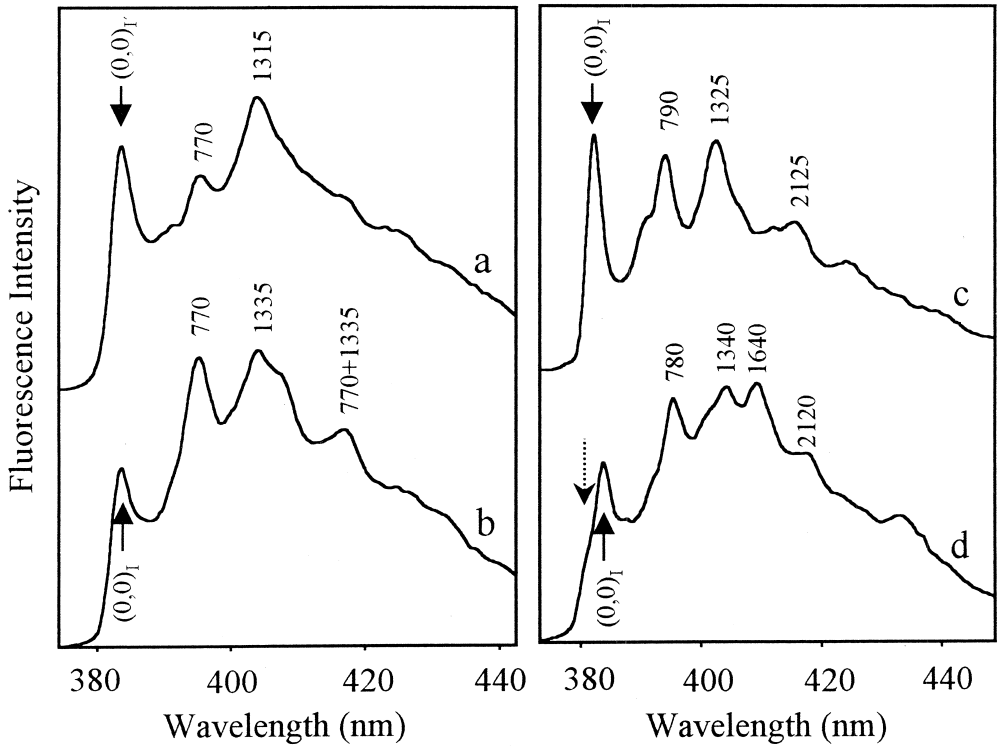

Fig. 3. NLN fluorescence spectra obtained off-line for (−)-*trans-anti*-DB[*a,l*]PDE-14-N^{6}dA (spectrum a), (−)-*cis-anti*-DB[*a,l*]PDE-N^{6}dA (spectrum b), (+)-*trans-syn*-DB[*a,l*]PDE-14-N^{6}dA (spectrum c), and (+)-*cis-syn*-DB[*a,l*]PDE-N^{6}dA (spectrum d) adducts in CE buffer. T=4.2 K, λ_{ex}=308 nm, delay time=80 ns, and gate width=200 ns. The numbers correspond to the ground state (S_0) vibrational frequencies.

being only weakly allowed [42,43]. With regard to spectrum c, we note that the *trans-syn*-dA adduct exists mostly in conformation I with its NLN spectra being weakly matrix and excitation-frequency dependent (data not shown). The conformation of the cyclohexenyl ring of the *trans-syn*-dA has been previously assigned as being a unique half-boat configuration with the dA moiety in a pseudoaxial position.[3] Finally, spectrum d of Fig. 3 is the NLN spectrum of the (+) *cis-syn*-adduct with a $(0,0)_I$ origin band at 383.5 nm. This adduct, in agreement with data previously obtained in ethanol and glycerol–water glasses [23], has been assigned as an open-type conformation with the cyclohexenyl ring in half-chair configuration and dA in a pseudoaxial position. A weak shoulder revealed in spectrum d of Fig. 3 for the (+)-*cis-syn*-dA adduct, denoted with a dashed arrow, corresponds to a decomposition product (presumably DB[*a,l*]tetrols) which is not observed in freshly synthesized samples. To generate a more accurate reference spectrum of the *cis-syn*-dA adduct, the decomposition product was electrokinetically separated from the adduct standard and an on-line reference spectrum of the ''pure'' *cis-syn*-dA standard was obtained as shown in Fig. 4.

3.2. Excitation and matrix dependent conformations

The existence of the conformations discussed above for the *trans-anti*-DB[*a,l*]PDE-14-N^{6}dA adducts is further confirmed below. Fig. 5 shows the NLN (T=77K) fluorescence dependence of this –dA adduct on excitation wavelength and matrix composition. Spectra a and c were obtained (off-line) in

Table 1
Fluorescence origin band comparison observed for *syn*- and *anti*-DB[*a,l*]PDE-14-N^{6}dA adducts at 77 and 4.2 K in various matrices (λ_{ex}=308 nm)

Stereoisomeric –dA adducts	Matrix					
	Ethanol[a]		Glycerol–water[a]		CE buffer	
	(0,0) nm	Conf.[b]	(0,0) nm	Conf.	(0,0)	Conf.
(+)-*trans-syn*-	382.0	**I**[c]	382.0	**I**	381.9	**I**
	389.0	II	389.0	II	–	–
(+)-*cis-syn*-	383.6	**I**	384.0	**I**	383.4	**I**
	388.0	II	388.0	II	–	–
(−)-*trans-anti*-	383.0	I′	–	I′	383.5	**I′**
	388.1	**II′**	388.3	**II′**	390.1[e]	II′
(−)-*cis-anti*-	385.0	I	385.0[d]	I	383.5	**I**
	389.0	**II**	389.0	**II**	–	–

[a] Observed at T=77 K with an excitation wavelength of 308 nm [23].
[b] Conf.=Conformation.
[c] The bold Roman numerals indicate the major conformations observed by low-temperature fluorescence.
[d] Minor conformation at the nucleoside level, but major conformation in single-stranded DNA [19].
[e] This origin band corresponds to the unique conformation II′ clearly revealed in CE buffer when selectively excited at 351.1 nm. The same conformation was also observed in an glycerol–CE matrix (80:20) (see Fig. 5 for details).

CE buffer with excitation wavelengths of 308 nm and 351.1 nm, respectively. An excitation wavelength of 308 nm preferentially excites adducts in conformation I′, with a (0,0) origin band at 383.5 nm, revealing characteristic bands at 770, 1315 and 2085 cm^{-1}. In contrast, an excitation wavelength of 351.1 nm preferentially excites adducts in conformation II′ with a (0,0) origin band at 390.1 nm, and vibrational bands at 750, 1280 and 2030 cm^{-1}. A small contribution of conformation II′ in spectrum a is also observed as denoted by an asterisk. Thus, we conclude that *trans-anti*-dA adducts exist in two conformations (I′ and II′), whose relative distribution is not only matrix dependent, but can also be revealed by selective laser excitation. The small difference in the intensity distribution between spectra a of Figs. 5 and 3 is due to a slightly different distribution of conformers I′ and II′ trapped at 4.2 and 77 K, respectively, and is the result of differences in cooling rates. The relatively strong bands at ~2085 cm^{-1} (curve a) and ~2030 cm^{-1} (curve c) correspond to the ~1315 and ~1280 cm^{-1} modes, which build on the intense Herzberg–Teller origin bands at 770 and 750 cm^{-1}, respectively; for more details see Ref. [21].

Spectrum b of Fig. 5 was obtained under conditions identical to those used to obtain spectrum a except that in a CE buffer–glycerol matrix (20:80, v/v). Comparison with spectrum a of Fig. 3 reveals that the (−)-*trans-anti*-dA adduct preferentially adopts conformation I′ in CE buffer and conformation II′ [(0,0) origin band at 389.6 nm] in the predominantly (80%) glycerol matrix. We emphasize that this conformation change is reversible (spectra not shown). Small differences in the vibronic intensity distribution observed in spectra b and c of Fig. 4 are caused by solvent (matrix) dependent Herzberg–Teller coupling [41,42]. Therefore, based on data presented in Fig. 5, we conclude that the *trans-anti*-DB[*a,l*]PDE-14-N^{6}dA adducts formed in CE buffer are trapped as a mixture of two adduct conformations. This provides additional support for the earlier assignment of these conformations as open- and folded-type, respectively. We recall that the cyclohexenyl ring in the above conformations possess a half-chair configuration with the dA moiety in a pseudoaxial and pseudoequatorial position, respectively [23]. Preliminary, matrix dependent, circular dichroism results support this assignment (data not shown).

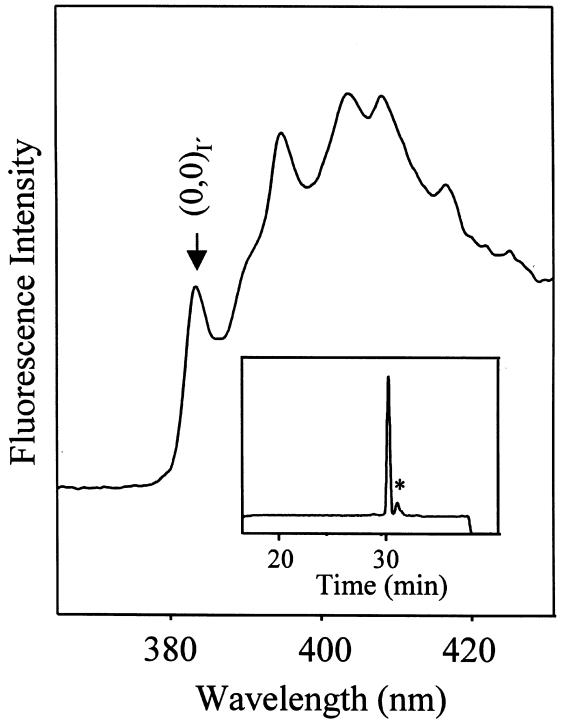

Fig. 4. On-line NLN fluorescence spectrum of "pure" (+)-*cis-syn*-DB[*a,l*]PDE-14-N^6dA. Inset, an electropherogram of the standard revealing the pure *cis-syn*-dA adduct (large peak) and a small contribution from a decomposition product (denoted with an asterisk). T=4.2K, λ_{ex}=308 nm, delay time=80 ns, and gate width=200 ns.

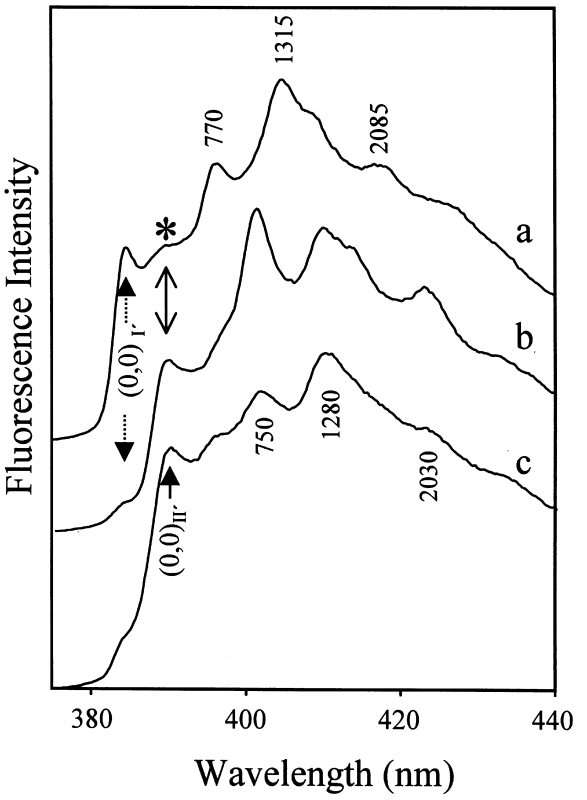

Fig. 5. Excitation wavelength and matrix dependence of the NLN fluorescence spectra of (−)-*trans-anti*-DB[*a,l*]PDE-14-N^6dA adducts at 77 K. Spectra a and c were obtained in CE buffer with an excitation wavelength of 308 nm and 351.1 nm, respectively. Spectrum b was obtained in the glycerol–CE buffer (80:20, v/v) solution with and λ_{ex}=308 nm. Spectra a and b were obtained with a 0 ns delay time and 200 ns observation window (see text for details).

3.3. CE separation

Despite considerable efforts, an electrokinetic separation of the –dA adducts was not achieved with either of the single surfactants, DOSS or Brij-S (data not shown). Therefore, we turned to mixed surfactant buffers, which were reported to be able to resolve structurally similar components that were inseparable under single surfactant conditions [44–46]. The buffer, which allowed for separation, consisted of 34.4 m*M* DOSS, 7.4 m*M* Brij-S, 6.8 m*M* sodium tetraborate, and 25.5% (v/v) acetonitrile. Altering the ratio of the two surfactants optimized electrophoretic resolution of the diastereomers. Utilizing the methodology described in Refs. [46,47], it was confirmed (data not shown) that at 25.5% acetonitrile, micelle formation was inhibited. This suggests that the CE separation mechanism involves a solvophobic association of the PAH portion of the DB[*a,l*]PDE-14-N^6dA adducts with the hydrophobic chains of the surfactants.

Separation of a mixture of eight diastereomeric –dA adducts is shown in Fig. 6. Since 11 peaks are nearly baseline resolved, three peaks of this electropherogram must belong to decomposition products or impurities.

3.4. On-line, low-temperature identification of CE-separated peaks

Fig. 7 shows the low-temperature (4.2 K) on-line

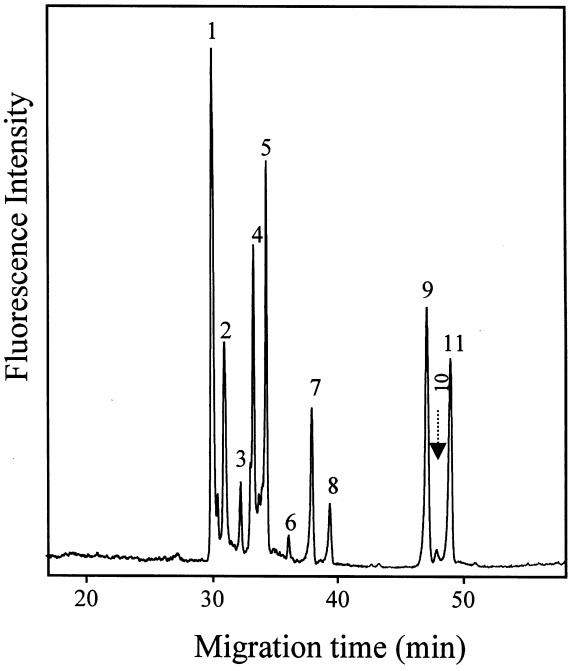

Fig. 6. Room-temperature fluorescence electropherogram acquired during CE separation of the eight HPLC purified DB[*a,l*]PDE-derived adduct standards. The peaks are identified in Table 2.

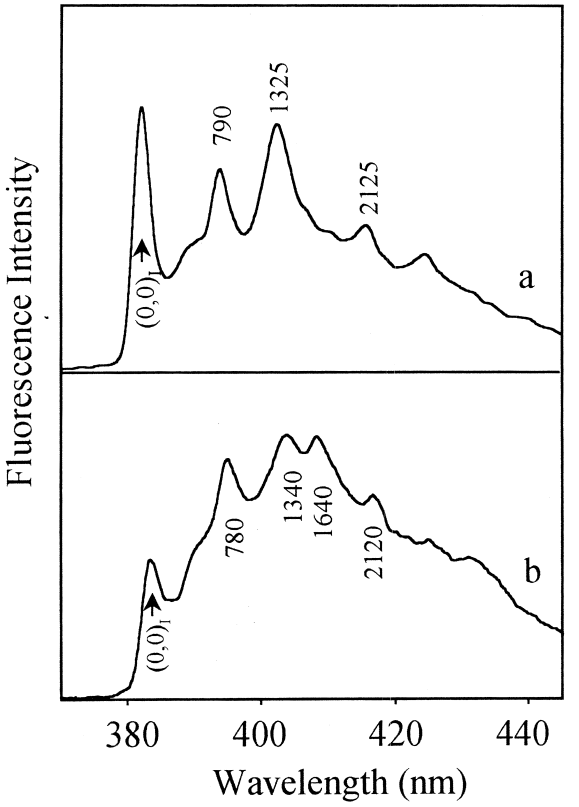

Fig. 7. On-line NLN spectra (a and b) for the CE-separated peaks 7 and 11 of Fig. 6. The bands are labeled with their ground-state vibrational frequencies, in cm^{-1}; T=4.2 K, λ_{ex}=308 nm.

spectral identification of peaks 7 (spectrum a) and 11 (spectrum b) of the electropherogram shown in Fig. 6. Peak identification is made based on comparisons with the library of the standard spectra. Spectrum a is identical to the off-line *trans-syn*-dA reference standard (spectrum c of Fig. 3), and spectrum b is indistinguishable from the spectrum in Fig. 4, which corresponds to the *cis-syn*-dA reference standard. Therefore, we conclude that peaks 7 and 11 of the electropherogram shown in Fig. 7 can be unambiguously assigned as the *trans-syn*- and *cis-syn*-DB[*a,l*]-PDE-14-N^6dA adducts, respectively.

Another example is shown in Fig. 8, where the identification of peaks 4 (spectrum a) and 5 (spectrum b) are illustrated. Both peaks reveal identical NLN spectra which are compared with the standard spectrum obtained for the (−)-*trans-anti*-dA (spectrum c). Since spectra a and b are nearly identical to the (−)-*trans-anti*-dA reference standard, we conclude that they must correspond to either the (+)- or (−)-*trans-anti*-DB[*a,l*]PDE-14-N^6dA diastereomers. The increased broadening observed in spectra a and b, as compared to the standard spectrum c, is a consequence of a slight reduction in spectral resolution (~1 nm) obtained in the on-line measurements. As mentioned earlier, and as discussed in Ref. [48], the (+)-*trans-anti*- and (−)-*trans-anti*-type adducts possess indistinguishable fluorescence spectra [22,23]. Their differentiation has been accomplished via spiking with optically pure standards whose stereochemistry has been established by ^{1}H NMR and circular dichroism [22]. The latter revealed that peaks 4 and 5 correspond to (+)-*trans-anti* and (−)-*trans-anti*-dA adducts, respectively. The same methodology of differentiating the (±) diastereomers was utilized for the remaining (±)-dA adduct pairs.

As a final example, Fig. 9 shows the on-line identification of the CE-separated peaks 7 and 11 of Fig. 6 via FLN spectroscopy. Frame A of Fig. 9

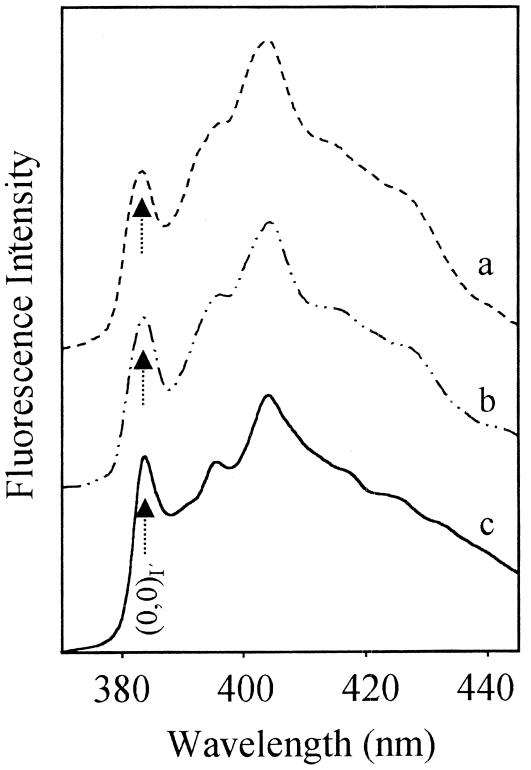

Fig. 8. Spectra a and b were obtained on-line in the CE–buffer matrix (at T=4.2 K, λ_{ex}=308 nm) for peaks 4 and 5, respectively, of Fig. 6. Spectrum c is from the library of NLN spectra and corresponds to the (−)-*trans*-*syn*-dA adduct. Spectra a, b and c were obtained with spectral resolution of 0.8 nm. The NLN bands are labeled with their ground-state vibrational frequencies, in cm^{-1}.

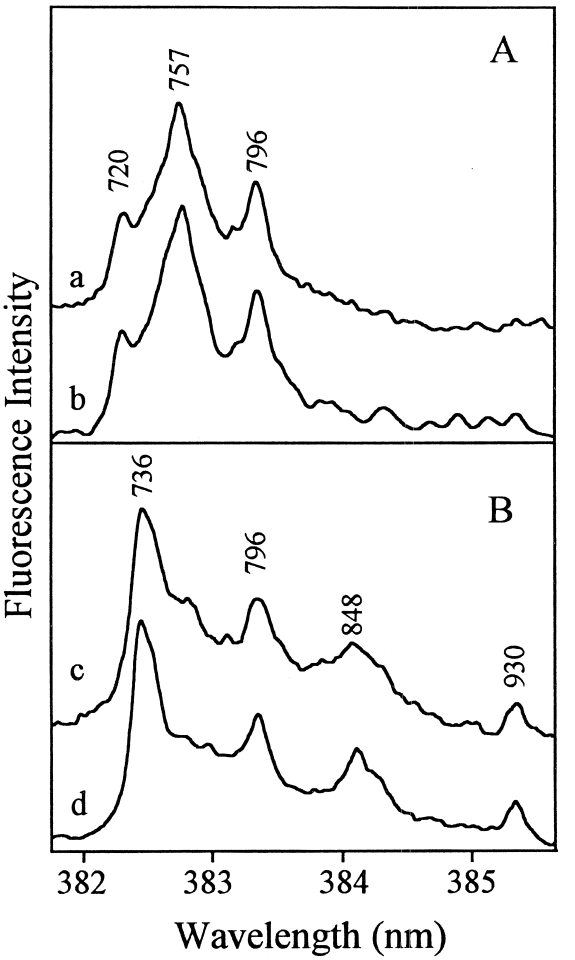

Fig. 9. Spectra a and c were obtained on-line in CE-buffer for peaks 7 and 11 of Fig. 6, with an excitation wavelength of 372.0 nm at T=4.2 K. Spectra b and d are shown for comparison, and corresponds to FLN spectra of the (+)-*trans*-*syn*- and (+)-*cis*-*syn*-DB[*a,l*]PDE-14-N^6dA adduct standards, respectively. The detection delay time was 40 ns with a 200 ns gate width. The FLN peaks are labeled with their excited-state vibrational frequencies, in cm^{-1}.

shows the 4.2 K FLN spectra (λ_{ex}=372.0 nm) of the CE-separated peak 7 (spectrum a) and the (+)-*trans*-*syn*-dA adduct standard (spectrum b). The comparison reveals vibronic modes at 720, 757 and 796 cm^{-1} in the on-line spectrum which are identical to those found in the (+)-*trans*-*syn*-dA adduct standard spectrum. Frame B of Fig. 9 compares the 4.2 K on-line FLN spectra (λ_{ex}=372.0 nm) of the CE separated peak 11 (spectrum c) with that of the off-line (+)-*cis*-*syn*-dA adduct standard (spectrum d). Again, identical vibrational modes at 736, 796, 848 and 930 cm^{-1} are observed, proving that peak 11 corresponds to the (+)-*cis*-*syn*-dA adduct. Thus, Figs. 7 and 9 demonstrate that *trans* and *cis* isomers of the *syn*-DB[*a,l*]PDE-14-N^6dA adducts are readily distinguishable and can be unambiguously assigned by both NLN and FLN spectra. The results obtained by combining CE with low-temperature fluorescence spectroscopy and spiking are summarized in Table 2.

4. Conclusions

The use of a capillary electrophoresis method for the separation and on-line spectral identification of

Table 2
The identity of the peaks in the electropherogram shown in Fig. 6

Peak No.	Peak assignment
1	(−)-*cis-anti*-DB[*a,l*]PDE-14-N^{6}dA
2	(+)-*cis-anti*-DB[*a,l*]PDE-14-N^{6}dA
3	Decomposition product
4	(+)-*trans-anti*-DB[*a,l*]PDE-14-N^{6}dA
5	(−)-*trans-anti*-DB[*a,l*]PDE-14-N^{6}dA
6	Decomposition product
7	(+)-*trans-syn*-DB[*a,l*]PDE-14-N^{6}dA
8	(−)-*trans-syn*-DB[*a,l*]PDE-14-N^{6}dA
9	(−)-*cis-syn*-DB[*a,l*]PDE-14-N^{6}dA
10	Decomposition product
11	(+)-*cis-syn*-DB[*a,l*]PDE-14-N^{6}dA

closely related analytes, via low-temperature fluorescence spectroscopy, has been demonstrated for diastereomeric dA adducts derived from the DB[*a,l*]-PDE. Successful separation of the eight stereoisomers was accomplished using an appropriate mixture of DOSS and Brij-S surfactants. Since the separation conditions inhibit micelle formation, it is concluded that the separation mechanism is the result of a solvophobic association of the PAH–dA adducts with the hydrophobic chains of the surfactants. It has been demonstrated that low-temperature CE–FNLN/FLN methodology not only allows for on-line identification via vibrationally resolved 4.2 K fluorescence spectra, but also provides conformational information on the –dA adducts. We believe that the marriage of CE to low-temperature fluorescence spectroscopy will be useful in future in vivo and in vitro studies of DNA adducts derived from DB[*a,l*]P and other fluorescent carcinogens.

5. Abbreviations

Ade, adenine
B[*e*]P, benzo[*e*]pyrene
CC, capillary cryostat
CCD, charge-coupled device
dA, deoxyadenosine
CE, capillary electrophoresis
CW, continuous wave
DB[*a,l*]P, dibenzo[*a,l*]pyrene
DB[*a,l*]PDE, dibenzo[*a,l*]pyrene diol epoxide
DB[*a,l*]PDE-14-N^{2}dG, dibenzo[*a,l*]pyrene diol epoxide-N^2-deoxyguanosine
syn-DB[*a,l*]PDE-14-N^{6}dA, *syn*-dibenzo[*a,l*]pyrene diol epoxide-14-N^{6}deoxyadenosine
anti-DB[*a,l*]PDE-N^{6}dA, *anti*-dibenzo[*a,l*]pyrene diol epoxide-14-N^{6}deoxyadenosine
DB[*a,l*]PDE-14-N7Ade, 14-(adenin-7-yl)-11,12,13-trihydroxy-11,12,13,14 tetrahydrodibenzo[*a,l*]-pyrene
DB[*a,l*]PDE-14-N7Gua, 14-(guanin-7-yl)-11,12,13-trihydroxy-11,12,13,14-tetrahydrodibenzo[*a,l*]pyrene
DB[*a,l*]P tetrol, 11,12,13,14-tetrahydroxy-11,12,13,14-tetrahydrodibenzo[*a,l*]pyrene
DE, diol epoxide
DOSS, dioctyl sulfosuccinate
FLNS, fluorescence line-narrowing spectroscopy
LIF, laser-induced fluorescence
NLN, non-line-narrowing
PAH, polycyclic aromatic hydrocarbon
S_0 state, electronic ground state
S_1 state, lowest excited singlet state

Acknowledgements

Iowa State University operates Ames Laboratory for the US Department of Energy under contract No. W-7405-Eng-82. The Office of Health and Environmental Research supported this research. C.-H. Lin was funded by the National Institutes of Health, grant POI CA49210-0. The authors thank E.L. Cavalieri for providing adduct standards and J.S. Fritz for the helpful discussions.

References

[1] K.-M. Li, R. Todorovic, E.G. Rogan, E.L. Cavalieri, F. Ariese, M. Suh, R. Jankowiak, G.J. Small, Biochemistry 34 (1995) 8043.
[2] E. Cavalieri, E. Rogan, A.H. Neilson (Ed.), The Handbook of Environmental Chemistry, PAHs and Related Compounds, Vol. 3, Springer, Berlin, Heidelberg, 1998, Part I.
[3] R. Jankowiak, G.J. Small, The Handbook of Environmental Chemistry, PAHs and Related Compounds, Vol. 3, Springer, Berlin, Heidelberg, 1998, Part I.
[4] E.L. Cavalieri, E.G. Rogan, Pharm. Ther. 55 (1992) 183.
[5] S.L. Ralston, A. Seidel, A. Luch, K.L. Platt, W.M. Baird, Carcinogenesis 16 (1995) 2899.
[6] A.H. Conney, Cancer Res. 42 (1982) 4875.
[7] A. Luch, H. Glatt, K.L. Platt, F. Oesch, A. Seidel, Carcinogenesis 15 (1994) 2507.

[8] R.G. Harvey, Polycyclic Aromatic Hydrocarbons – Chemistry and Carcinogenicity, Cambridge University Press, Cambridge, 1991.
[9] S.L. Ralston, H.H.S. Lau, A. Seidel, A. Luch, K.L. Platt, W.M. Baird, Cancer Res. 54 (1994) 887.
[10] K.-M. Li, N.V.S. RamaKrishna, N.S. Padmavathi, E.G. Rogan, E.L. Cavalieri, Polycyclic Aromat. Comp. 6 (1994) 207.
[11] D. Chakravarti, R. Mailander, J. Franzen, S. Higgenbotham, E.L. Cavalieri, E.G. Rogan, Oncogene 16 (1998) 3203.
[12] D. Chakravarti, E.L. Cavalieri, E.G. Rogan, DNA Cell Biol. 17 (1998) 529.
[13] E.L. Cavalieri, S. Higginbotham, N.V.S. RamaKrishna, P.D. Devaneasan, R. Todorovic, E.G. Rogan, S. Salmasi, Carcinogenesis 12 (1991) 1939.
[14] S. Higginbotham, N.V.S. RamaKrishna, S.L. Johansson, E.G. Rogan, E.L. Cavalieri, Carcinogenesis 14 (1993) 875.
[15] I.S. Kozin, C. Gooijer, N.H. Velthorst, Anal. Chem. 67 (1995) 1623.
[16] J.L. Mumford, X. Li, F. Hu, X.B. Lu, J.C. Chuang, Carcinogenesis 16 (1995) 3031.
[17] W.K. deRatt, S.A.L.M. Kooijman, J.W.J. Gielen, Sci. Total Environ. 66 (1987) 95.
[18] R. Jankowiak, D. Zamzow, W. Ding, G.J. Small, Anal. Chem. 68 (1996) 2549.
[19] R. Jankowiak, F. Ariese, A. Hewer, A. Luch, D. Zamzow, N.C. Hughes, D. Phillips, A. Seidel, K.L. Platt, F. Oesch, G.J. Small, Chem. Res. Toxicol. 11 (1998) 674.
[20] F. Ariese, G.J. Small, R. Jankowiak, Carcinogenesis 17 (1996) 829.
[21] R. Jankowiak, F. Ariese, D. Zamzow, A. Luch, H. Kroth, A. Seidel, G.J. Small, Chem. Res. Toxicol. 10 (1997) 677.
[22] K.-M. Li, E.L. Cavalieri, E.G. Rogan, M. George, M.L. Gross, A. Seidel, Chem. Res. Toxicol., in press
[23] R. Jankowiak, C.-H. Lin, D. Zamzow, K. Roberts, K.-M. Li, G.J. Small, Chem. Res. Toxicol., in press
[24] D. Zamzow, C.-H. Lin, G.J. Small, R. Jankowiak, J. Chromatogr. A 781 (1997) 73.
[25] D. Zamzow, G.J. Small, R. Jankowiak, Mol. Cryst. Liq. Cryst. 291 (1996) 155.
[26] S. Pleasance, S.W. Ayer, M.V. Laycock, P. Thibault, Rapid Comm. Mass Spectrom. 6 (1992) 14.
[27] W. Lu, G.K. Poon, P.L. Carmichael, R.B. Cole, Anal. Chem. 68 (1996) 668.
[28] H. Ozaki, N. Itou, S. Terabe, T. Takada, M. Sakairi, H. Koizumi, J. Chromatogr. A 716 (1995) 69.
[29] J. Cai, J. Henion, J. Anal. Toxicol. 20 (1996) 27.
[30] S.J. Locke, P. Thibault, Anal. Chem. 66 (1994) 3436.
[31] J. Cai, J. Henion, J. Chromatogr. A 703 (1995) 667.
[32] D.L. Olson, M.E. Lacey, J.V. Sweedler, Anal. Chem. 70 (1998) 257A.
[33] V. Pretoris, B.J. Hopkins, J.D. Schieke, J. Chromatogr. 99 (1974) 23.
[34] J.W. Jorgenson, K.D. Lukacs, J. Chromatogr. 218 (1981) 209.
[35] J. Ding, P. Vouros, Am. Lab. 30 (1998) 15.
[36] K.P. Roberts, R. Jankowiak, G.J. Small, in preparation.
[37] S.J. Kok, E.M. Kristensons, C. Gooijer, N.H. Velthorst, U.A.Th. Brinkman, J. Chromatogr. A 771 (1997) 331.
[38] R. Jankowiak, G.J. Small, Chem. Res. Toxicol. 4 (1991) 256.
[39] R. Jankowiak, J.M. Hayes, G.J. Small, Chem. Rev. 93 (1993) 1471.
[40] W. Ding, J.S. Fritz, Anal. Chem. 69 (1997) 1593.
[41] J.C. Brown, J.A. Duncanson, G.J. Small, Anal. Chem. 52 (1980) 1711.
[42] G. Herzberg, Molecular Spectra and Molecular Structure, III. Electronic Spectra and Electronic Structure of Polyatomic Molecules, Van Nostrand and Reinhold, New York, 1966, Ch. 2.
[43] J.C. Brown, Ph.D. Thesis, Iowa State University, Ames, IA, p. 131.
[44] X. Li, J.S. Fritz, Anal. Chem. 68 (1996) 4481.
[45] S.K. Poole, C.F. Poole, J. High Resolut. Chromatogr. 20 (1997) 174.
[46] J.H.T. Luong, Y. Guo, Electrophoresis 19 (1998) 723.
[47] C.C. Ruiz, Coll. Poly. Sci. 273 (1995) 1033.
[48] M. Suh, F. Ariese, G.J. Small, R. Jankowiak, T.-M. Liu, N.E. Geacintov, Biophys. Chem. 56 (1995) 281.